3 Discovery of a selective PPARδ agonist

3.1 Objective

Though PPARδ was discovered soon after the discovery of PPAR*α* and PPARγ it remained unexplored till last few years. Over two decades of the research efforts to develop PPAR*α* or/and γ agonists were not able to deliver the success. Probably this had created an attention of the drug discovery scientists all over the globe towards PPAR*δ* isoform. Targeting PPAR*δ* is established as a new approach to PPAR research for the treatment of metabolic syndrome and inflammation. Recently it has been identified that like the other two isoforms PPAR*δ* is also involved in various aspects of lipid metabolism, cell differentiation and inflammation. As PPAR*δ* is associated with adipogenesis it may be a potential target for treating obesity and related disorders. It also has been identified that PPAR*δ* has an important role in controlling lipid metabolism by

raising HDL level and lowering LDL and triglycerides. PPARδ receptor may also be critically involved in insulin resistance.

The role of PPAR*δ* in regulating inflammation and immunity is not yet completely understood. It has recently been identified that PPAR*δ* regulates several inflammatory genes such as MCP-5, IL-1β, TNFα, IL-6 and VCAM-1. However the clinical proof of concept is still awaited as very few PPAR*δ* selective agonists are in the clinical trials.

In contrast to PPAR*α* and PPARγ, there are no PPAR*δ* agonists in the market. However, in view of the emerging functions of this unexplored member of the PPARs, PPAR*δ* agonists are likely to promote beneficial effects on dyslipidaemia associated with metabolic syndrome X and inflammation. Based on these findings, it was intended to investigate for the development of a selective PPAR*δ* agonist.

3.2 Designing Strategy

Emerging role of PPAR*δ* in metabolic syndrome intrigued the interest to develop PPARδ agonists for the treatment of inflammation and cardiovascular diseases related to complex metabolic syndrome. As a part of the research program directed towards the development of novel PPAR ligands,[157-161,166,167] a PPAR pan agonist **11a** was developed with potent hypolipidemic and anti-hyperglycemic activities.[168] During that study, it was observed that PPARδ selectivity increased when bulkier group like cyclohexyl is introduced on oxime ether part (compound **11f),** (Figure 20). In-silico studies on this scaffold further revealed that PPARδ selectivity is very sensitive to the size of the substituent on oxime ether part. For the fact that ligand binding pocket of PPARδ is smaller than PPAR α and γ, it was needed that the thiazole ring is omitted from the lipophilic part to make the molecule comparatively smaller in length. Keeping these in mind a novel series of compounds **56a-k** with bulky substitution on oxime ether was designed (Figure 20).

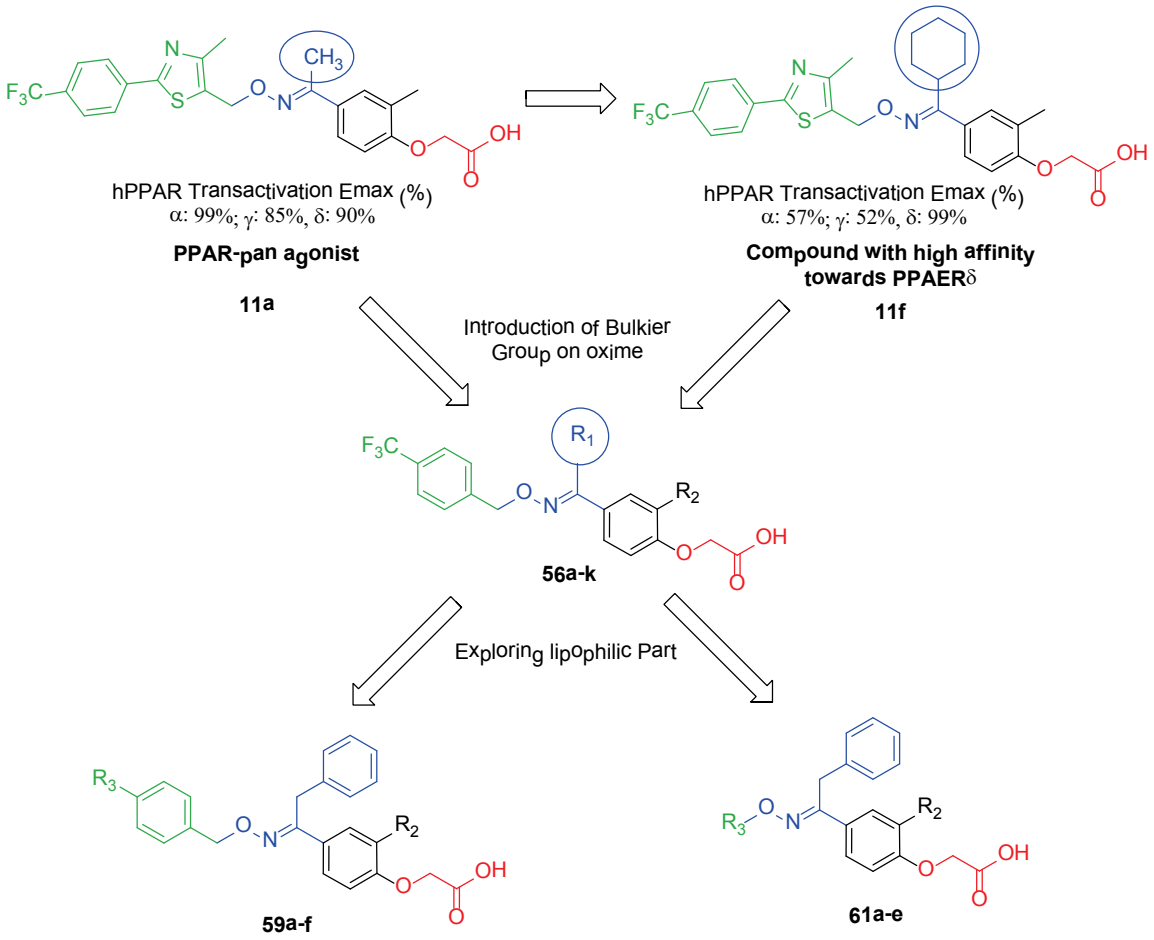

Figure 20: Designing PPARδ agonist

Having studied various bulkier groups on oxime (**56a-k)** to explore the role of chemical spacer in lipophilic part and compounds **59a-f** and **61a-e** containing various substitutions on lipophilic aryl group and possessing various heterocyclic group respectively were designed as shown in Figure 20.

3.3 Results and discussion

3.3.1 Chemistry

Oxime intermediates **54a-e** containing bulkier group at R_1 were synthesized as shown in Scheme 15.

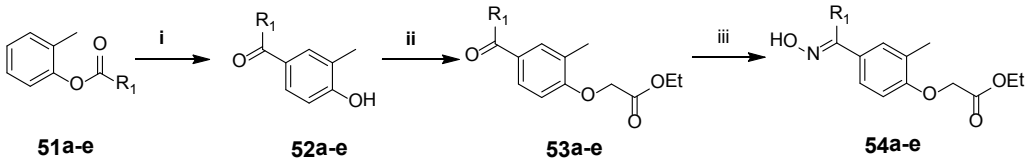

51a-e 52a-e 53a-e 54a-e

Compound	54a	54b	54c	54d	54e
R_1	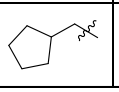	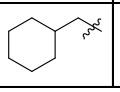	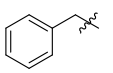	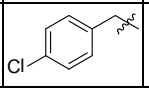	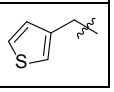

Scheme 15: Reagents and conditions: (i) anhydrous $AlCl_3$, 160 ^oC, 2 h; (ii) Ethyl chloroacetate, K_2CO_3, DMF, 60 ^oC, 18 h; (iii) $NH_2OH.HCl$, CH_3COONa, Ethanol, reflux, 1 h

Starting materials **51a-e** were synthesized by reacting *o*-cresol and respective acid chlorides in the presence of triethylamine in dichloromethane. Fries rearrangement of compounds **51a-e** using anhydrous $AlCl_3$ resulted in 4-acylphenols **52a-e** which upon treatment with ethyl chloroacetate and potassium carbonate in DMF gave the intermediate **53a-e**. The oxime preparation was carried out by the treatment of compounds **53a-e** with hydroxylammonium chloride and sodium acetate in ethanol giving the oximes **54a-e**.

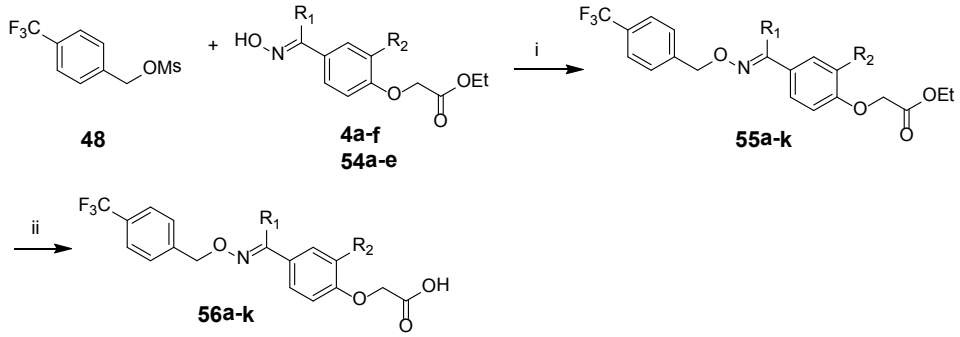

48 4a-f 54a-e 55a-k 56a-k

Compound	56a	56b	56c	56d	56e	56f	56g	56h	56i	56j	56k
R_1	Me	Me	Et	Et	*n*-Pr		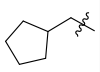	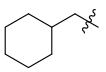	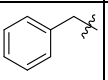	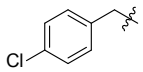	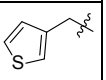
R_2	Me	H	Me	H	Me	Me	Me	Me	Me	Me	Me

Scheme 16: Reagents and conditions: (i) Cs_2CO_3, DMF, 60 ^oC, 3 h; (ii) $LiOH.H_2O$, THF, methanol, H_2O, 25 ^oC, 18 h

Nucleophilic substitution reaction on the mesylate **48** with oximes **4a-f** & **54a-e** with cesium carbonate in DMF under nitrogen atmosphere yielded esters

55a-k. Further hydrolysis of esters **55a-k** by lithium hydroxide gave corresponding acids **56a-k** (Scheme 16).

Based on the biological activity results of the compounds **56a-k** another series of compounds **59a-f** was designed and synthesis was carried out as depicted in Scheme 17.

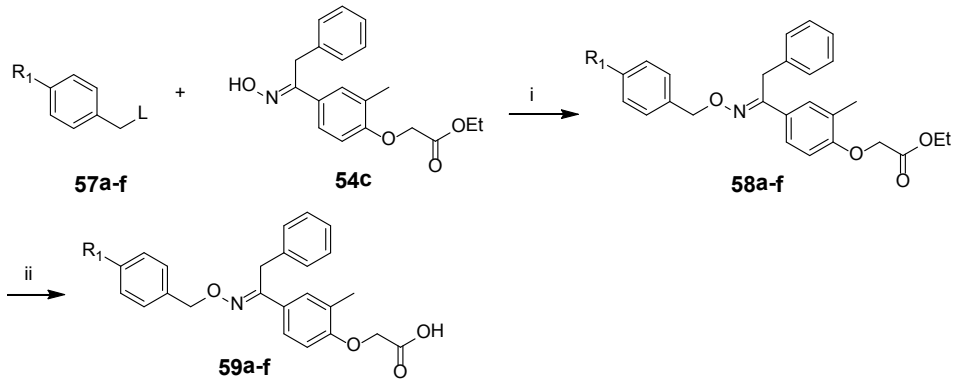

Compound	59a	59b	59c	59d	59e	59f
R_1	H	Me	OMe	OCF_3	Cl	F
L	Cl	OMs	OMs	Br	Cl	Cl

Scheme 17: Reagents and conditions: (i) Cs_2CO_3, DMF, 60 ^oC, 3 h; (ii) $LiOH.H_2O$, THF, methanol, H_2O, 25 ^oC, 18 h

Starting materials **57a-f** were either procured from commercial source or prepared from their corresponding benzyl alcohols by reacting with methanesulfonyl chloride in presence of triethylamine. Treatment of the intermediates **57a-f** and oxime **54c** in the presence of cesium carbonate in DMF under nitrogen atmosphere yielded esters **58a-f** which on hydrolysis using lithium hydroxide resulted in the acids **59a-f** in good yield.

To study the lipophilic part more extensively compounds **61a-e** with various lipophilic heterocycles were designed and synthesized as illustrated in Scheme 18. Synthesis of heterocyclic intermediates **9**, **17** and **34a-b** is described in sections 2.2.2.1, 2.3.2.1 and 2.4.2.1 respectively. These intermediates were reacted with oxime **54c** and cesium carbonate and after purification through

column chromatography the resulting esters **60a-e** were subjected for hydrolysis by lithium hydroxide to give final compounds **61a-e**.

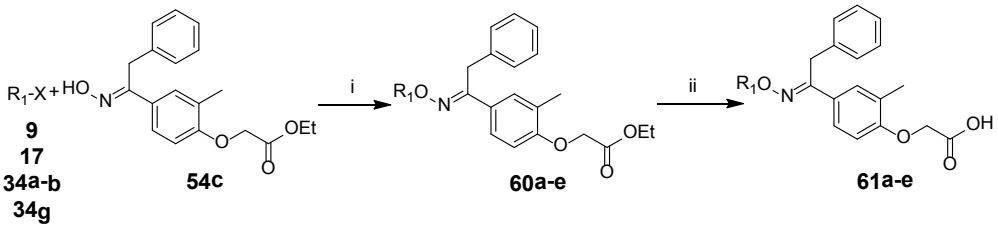

Compound	61a	61b	61c	61d	61e
R_1	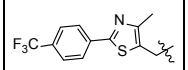	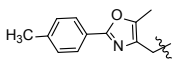	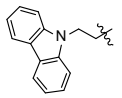	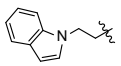	
X	Cl	Cl	OMs	OMs	Cl

Scheme 18: Reagents and conditions: (i) Cs_2CO_3, DMF, 60 ^oC, 18 h; (ii) $LiOH.H_2O$, THF, methanol, H_2O, 25 ^oC, 18 h

The detailed synthetic procedures and characterization data are described in the experimental section. Physical, analytical and spectral data of all the final as well as intermediate compounds are in conformity with the structures assigned.

3.3.2 *In vitro* PPAR transactivation

The newly synthesized compounds **56a-k**, **59a-f** and **61a-e** were screened for human PPAR (hPPAR) α, γ and δ agonistic activities on full length PPAR receptor transfected in HepG2 cells as described in the experimental section. WY-14643, Rosiglitazone and GW-501516 were used as positive controls for PPAR α, γ and δ respectively. The in vitro PPAR subtype agonistic activities are reported as percent maximal activity of each compound compared to reference compound and normalized to 100%.

During the study of modulating PPAR subtypes selectivity by introducing structurally constrained oxime ether linker it was observed that the groups which occupy more space on oxime linker are favorable for PPARδ selectivity. While studying lipophilic part it was also noticed that trifluoromethyl substituted phenyl

ring is suitable for PPAR affinity. Keeping this observation in mind to achieve the goal of getting selective PPARδ agonist the compounds **56a-k** with varried substitution on oxime were synthesized. All the compounds were subjected for *in vitro* PPAR transactivation essay and results of that are described in Table 15.

Table 15: In vitro PPAR agonistic activity of test compounds **56a-k**.

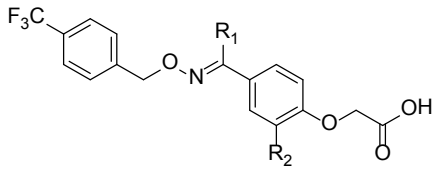

Compound	R_1	R_2	hPPAR Transactivation E_{max} (%)[a, b]		
			α	γ	δ
56a	Me	Me	86.2 ± 1.9	96.3 ± 3.6	108.0 ± 8.9
56b	Me	H	51.5 ± 3.2	53.5 ± 2.8	105.1 ± 5.1
56c	Et	Me	75.4 ± 5.1	130.9 ± 9.3	165.4 ± 3.2
56d	Et	H	81.3 ± 6.2	51.4 ± 4.5	69.9 ± 1.9
56e	Pr	Me	13.9 ± 2.3	13.3 ± 0.9	29.3 ± 2.9
56f		Me	20.2 ± 1.0	43.9 ± 4.9	81.8 ± 4.0
56g	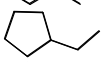	Me	8.6 ± 1.6	14.1 ± 2.8	14.2 ± 4.4
56h	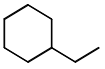	Me	32.0 ± 3.2	35.8 ± 3.1	62.3 ± 7.3
56i	Benzyl	Me	11.8 ± 1.8	13.9 ± 1.9	48.5 ± 5.2
56j	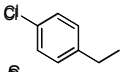	Me	4.3 ± 1.1	3.3 ± 1.0	98.3 ± 6.4
56k	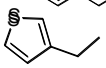	Me	1.1 ± 0.6	3.4 ± 1.4	4.5 ± 2.8
GW 501516@ 2 nM			76.9 ± 7.1	61.1 ± 2.4	100.4 ± 4.3

[a]HepG2 cells transfected with pSG5 expression vector containing the cDNA of hPPARα or hPPARγ or hPPARδ and cotransfected with PPRE3-TK-luc. The luciferase activity determined using fire-fly luciferase assay and β-galactosidase activity determined in ELISA reader (n=3).

[b]E_{max} of test compounds compared to reference compounds (WY-14643 for α, Rosiglitazone for γ and GW-501516 for δ) normalized to 100%. Fold increase of WY-14643, Rosiglitazone and GW-501516 Vs DMSO is 8.40 ± 0.21 (PPARα), 13.49 ± 0.38 (PPARγ) and 28.54 ± 0.77 (PPARδ) respectively at 10 μM concentration.

PPAR activity of the compounds **56a-f** followed the trend shown by the similar series of compounds in the previous chapter. Compounds **56a** and **56c** possessing methyl and ethyl group respectively as R_1 activate all three subtypes

of PPARs. Whereas removal of the methyl group from the *ortho* position of the central aromatic ring as exemplified by the compounds **56b** and **56d** resulted in decreasing PPAR activity. Further increase in the chain length of R1 found detrimental to PPAR affinity as shown by compound **56e**. As hypothesized PPARδ selectivity increased when bulkier cyclohexyl group was introduced as R_1 as seen in Table 15. These results intensified to study various bulkier substitutions on oxime linker and compounds **56g-f** with bulkier group as R_1 were synthesized. When cyclohexyl group was replaced by cyclopentylmethyl the resulting compound **56g** did not show PPAR activation. Further ring enlargement from cyclopentylmethyl to cyclohexylmethyl group increased PPARδ affinity as shown by **56h**. In order to greater PPARδ selectivity cyclohexylmethyl group was replaced by benzyl group on oxime linker in compound **56i** which showed moderate efficacy towards PPARδ and came out as first PPARδ selective agonist with no affinity towards PPARα and PPARγ among this class of compounds (E_{max} (%) of 11.8 ± 1.8, 13.9 ± 1.9 and 48.5 ± 5.2 for α, γ and δ respectively). Compound **56j** having 4-chlorobenzyl group was also found to be highly selective to PPARδ (E_{max} (%) of 4.3 ± 1.1, 3.3 ± 1.0 and 98.3 ± 6.4 for α, γ and δ respectively) however compound **56k** with thiophene group did not show any activity. These results proved the hypothesis of advantage of bulkier substitution on oxime linker to obtain PPARδ selective agonist. From these results it has also been observed that aryl ring system on oxime linker is more suitable for selectivity towards PPARδ rather than cycloalkyl or heterocyclic substitution.

Based on the above results compounds **56i** and **56j** were selected for EC_{50} determination whose results are included in Figure 21. As can be observed in Figure 21 compound **56i** was found as a partial PPARδ agonist with EC_{50} of 0.43 μM whereas compound **56j** was identified as a full PPARδ agonist with EC_{50} of 5.9 μM.

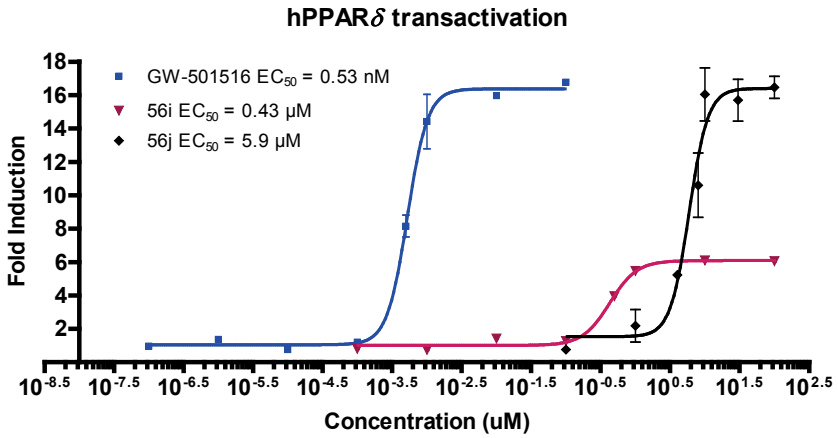

Figure 21: EC_{50} of selected test compounds **56i** and **56j**

HepG2 cells transfected with pSG5 expression vector containing the cDNA of hPPARδ and cotransfected with PPRE3-TK-luc. The luciferase activity determined using fire-fly luciferase assay and β-galactosidase activity determined in ELISA reader.

Further to confirm the selectivity of compound **56i**, fold induction study was carried out as represented in Figure 22.

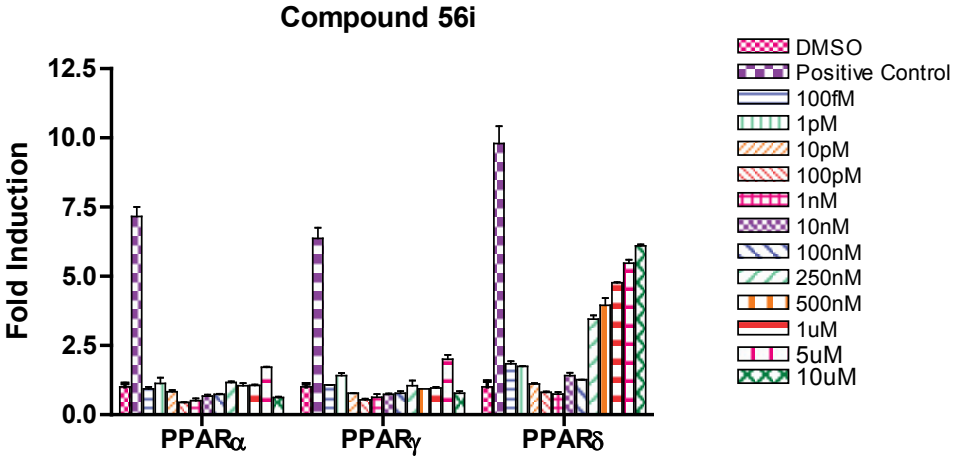

Figure 22: Fold induction Vs DMSO of Compound **56i**

HepG2 cells transfected with pSG5 expression vector containing the cDNA of hPPARα or hPPARγ or hPPARδ and cotransfected with PPRE3-TK-luc. The luciferase activity determined using fire-fly luciferase assay and β-galactosidase activity determined in ELISA reader (n=3). Activities are presented as fold induction of PPARα, γ and δ activation over the basal level (DMSO).

Fold induction versus vehicle control 1% DMSO solution was measured at different concentrations ranging from 100 fM to 10 µM of test compound **56i** for

PPAR *α*, *γ* and *δ*. Compound **56i** demonstrated dose dependent increase in activation of PPAR*δ* but did not show any activation of PPAR *α* and *γ* when tested in different concentrations (Figure 22).

Having encouraged with the results it was planned to study modification of lipophilic part. In an attempt to identify the role of substitutions on the lipophilic phenyl ring, compounds **59a-f** with different kind of substitutions on phenyl ring were synthesized. All the compounds were tested in hPPAR transactivation assay and the data is described in Table 16.

Table 16: In vitro PPAR agonistic activity of test compounds **59a-f**.

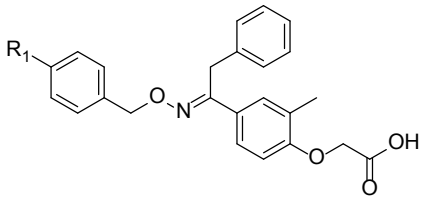

Compound	R_1	hPPAR Transactivation E_{max} (%) [a,b]		
		α	*γ*	*δ*
56i	CF_3	11.3 ± 1.3	13.2 ± 0.9	48.3 ± 2.3
59a	H	65.0 ± 2.4	70.7 ± 4.2	145.5 ± 12.2
59b	Me	37.3 ± 3.7	12.5 ± 3.1	35.6 ± 1.9
59c	OMe	70.3 ± 3.0	38.8 ± 1.9	91.9 ± 6.8
59d	OCF_3	<1	<1	<1
59e	Cl	5.1 ± 1.2	7.0 ± 1.1	12.7 ± 3.2
59f	F	47.2 ± 3.9	37.9 ± 4.4	75.7 ± 2.4
GW 501516@ 2 nM		76.9 ± 7.1	61.1 ± 2.4	100.4 ± 4.3

[a]HepG2 cells transfected with pSG5 expression vector containing the cDNA of hPPAR*α* or hPPAR*γ* or hPPAR*δ* and cotransfected with PPRE3-TK-luc. The luciferase activity determined using fire-fly luciferase assay and *β*-galactosidase activity determined in ELISA reader (n=3).

[b]E_{max} of test compounds compared to reference compounds (WY-14643 for *α*, Rosiglitazone for *γ* and GW-501516 for *δ*) normalized to 100%. Fold increase of WY-14643, Rosiglitazone and GW-501516 Vs DMSO is 8.40 ± 0.21 (PPARα), 13.49 ± 0.38 (PPARγ) and 28.54 ± 0.77 (PPARδ) respectively at 10 µM concentration.

Compound **59a** without any substitution on phenyl ring found to activate PPAR *α, γ* and *δ*. However compound **59b** with methyl substituent at position-4

found to be mild activator of PPAR *α* and δ but no activation of hPPARγ was observed. Similar to compound **59a** compounds **59c** and **59f** with 4-methoxy and 4-fluoro group respectively exhibited significant PPARδ activity with no selectivity over other subtypes. Surprisingly *para* substitution on phenyl with 4-trifluoromethoxy and 4-chloro group as exemplified by compounds **59d** and **59e** respectively resulted in complete loss of activity. So here we conclude that 4-CF_3 is the most suited substitution for PPARδ selectivity.

As a part of SAR study the compounds **61a-e** were designed by replacing trifluoromethyl substituted phenyl ring of compound **56i** by various heterocycles based on the earlier results discussed in the previous chapter. All the test compounds were analyzed by *in vitro* PPAR transactivation essay for their PPAR agonistic activity. Initially thiazole and oxazole heterocycles were selected which were present as a lipophilic part in pervious active series and compounds **61a** and **61b** were synthesized respectively. In contrary to the earlier results, introduction of these heterocycles resulted in reduction of PPAR activity as shown in Table17.

Table 17: In vitro PPAR agonistic activity of test compounds **61a-e**

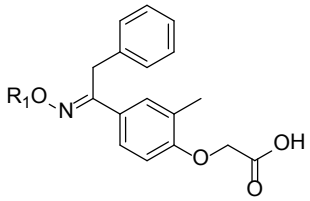

Compound	R_1	hPPAR Transactivation[a,d] E_{max} (%)[b]		
		α	*γ*	*δ*
61a	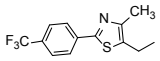	16.0 ± 2.3	17.2 ± 0.8	26.6 ± 1.6
61b	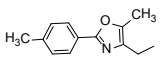	22.1 ± 2.9	56.1 ± 5.1	25.5 ± 1.9

Compound	R_1	hPPAR Transactivation[a,d] E_{max} (%)[b]		
		α	γ	δ
61c	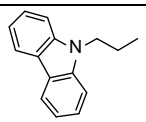	<1	<1	<1
61d	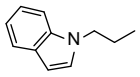	42.3 ± 3.2	17.5 ± 2.5	40.4 ± 4.4
61e		80.8 ± 1.8	48.6 ± 6.6	68.2 ± 8.4
GW 501516@ 2 nM		76.9 ± 7.1	61.1 ± 2.4	100.4 ± 4.3

[a]HepG2 cells transfected with pSG5 expression vector containing the cDNA of hPPARα or hPPARγ or hPPARδ and cotransfected with PPRE3-TK-luc. The luciferase activity determined using fire-fly luciferase assay and β-galactosidase activity determined in ELISA reader (n=3).
[b]E_{max} of test compounds compared to reference compounds (WY-14643 for α, Rosiglitazone for γ and GW-501516 for δ) normalized to 100%. Fold increase of WY-14643, Rosiglitazone and GW-501516 Vs DMSO is 8.40 ± 0.21 (PPARα), 13.49 ± 0.38 (PPARγ) and 28.54 ± 0.77 (PPARδ) respectively at 10 µM concentration.

Compounds containing N-linked bicycle indole and tricyclic carbazole as demonstrated by compounds **61c** and **61d** also failed to show PPAR activation. Whereas compound **61e** possessing ortho-fluorobenzyl group showed moderate activation of PPARs but selectivity was missing. These results indicate the importance of aryl group in this scaffold for PPAR affinity. From these data we also conclude that heterocyclic groups in this scaffold are not suitable for having PPAR activity.

From all the *in vitro* results of these three series we identified compound **56i** as a partial and selective PPARδ agonist whereas compound **56j** was found to be full agonist of PPARδ with a high degree of selectivity among all three PPAR subtypes. Though compound **56j** possesses a high selectivity towards PPARδ, it shows very low potency of 5.9 µM (EC_{50}). And because of that it may require a high dose to show the activity in *in vivo* experiments. Hence compound **56i** was selected for further *in vivo* experiments in selected animal models.

3.3.3 *In vivo* evaluation

In vivo studies of the compound **56i** were carried out in order to evaluate its anti-hyperglycemic and anti-inflammatory activities. Detailed experimental procedures of *in vivo* studies are described in the experimental section.

As PPARδ is known to play a key role in insulin resistance and lipid metabolism we decided to study compound **56i** in male *db/db* mice to assess its anti-hyperglycemic activity. Compound **11a** was dosed orally (po) at 10 mpk/day and 30 mpk/day for 14 days and the results are schematically presented in Figure 23.

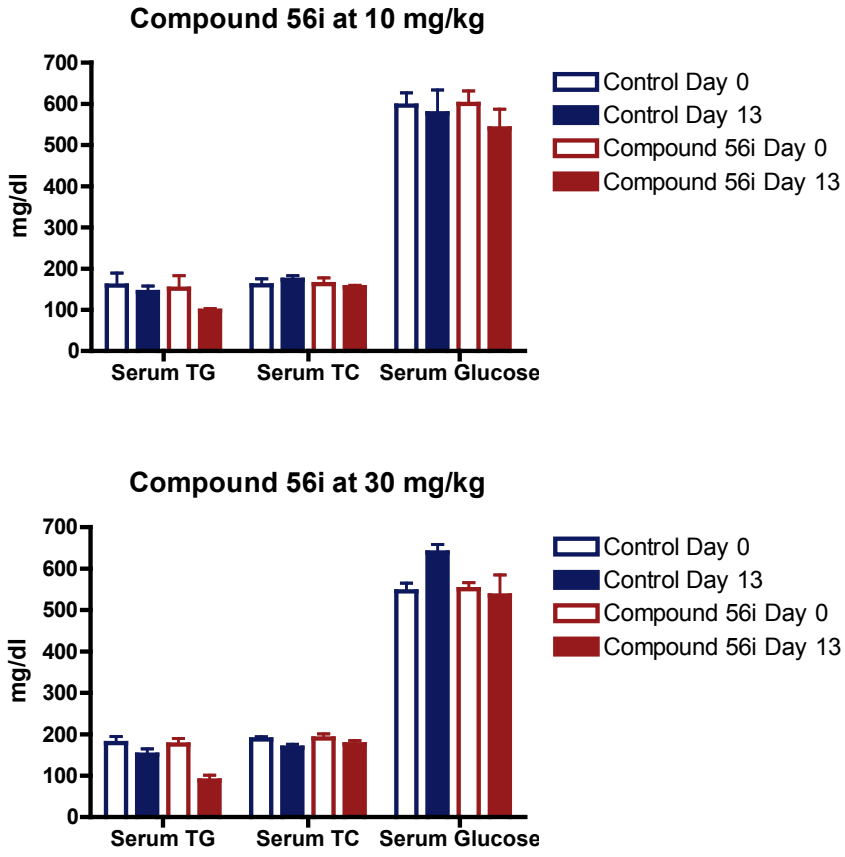

Figure 23: Anti-hyperglycemic activity of the selected compound **56i** in *db/db* mice
Male *db/db* mice dosed orally (po) with test compounds daily for 14 days and serum glucose, triglycerides (TG) and total cholesterol were measured. Values expressed as % change of compound-treated mice vs vehicle control, indicated as M±SD (n=6), significant at $p < 0.05$.

Surprisingly the test compounds **56i** did not show any reduction in serum glucose, serum triglyceride and serum total cholesterol. This result indicates that compound **56i** is not affecting metabolic levels at 10 mpk/day and 30 mpk/day dose in *db/db* mice.

In order to study the anti-inflammatory activity, the compound **56i** was tested for LPS induced end toxemia in *Swiss albino mice* (SAM) and BALB/c mice at 100 mg/kg dose. The activity was measured as reduction in the levels of TNF-*α* and IL-6 compare to the control group. The results are included in Table 18. In contrast to the results of *db/db* mice, the compound **56i** demonstrated significant TNFα reduction of 63% and 37% in *SAM* and *BALB/c* mice respectively. Compound **56i** also showed good reduction in IL-6 in *SAM* but unable to show IL-6 reduction in *BALB/c* mice.

Table 18: LPS induce endotoxemia of test compound **56i** in SAM and BALB/c mice[a]

Compound	Swiss albino mice		Balb/c mice	
	% Change TNFα[a]	% Change IL-6[b]	% Change TNFα[b]	% Change IL-6[b]
4508	-63.0 ± 8.5	-27.0 ± 8.0	-36.9 ± 6.0	-3.0 ± 4.1

[a]The animals were dosed orally (po) with test compounds or vehicle 1 hour prior to the intravenous injection of LPS. The level of TNFα (1 hour after administration of LPS) and IL-6 (1 hour after administration of LPS) were measured.
[b]Values expressed as % change of compound-treated mice vs vehicle control.

To optimize the dose, the same study was performed in *SAM* at three different doses. The compound **56i** showed dose dependent reduction in TNF*α*. At 10 mg/kg dose no reduction in TNF*α* was observed whereas compound **56i** effectively reduced TNF*α* at 30 mg/kg and 100 mg/kg doses (32% and 63% reduction respectively) (Figure 24).

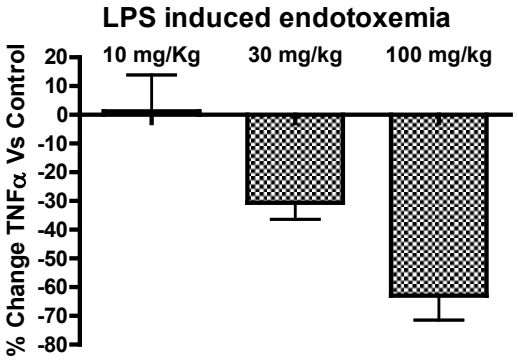

Figure 24: LPS induce endotoxemia of compound **56i** in *SAM*

Overall the *in vivo* results indicate that the selective PPARδ partial agonist **56i** possesses promising anti-inflammatory properties without altering metabolic levels in rodents. These results also reveal sPPARM like properties of the compound **56i** which exhibits the therapeutic effects of PPARδ in a selective manner. In order to validate sPPARM properties of compound **56i**, gene expression studies need to be carried out.

3.3.4 Pharmacokinetic study

In order to understand pharmacokinetic behavior of compound **56i** the pharmacokinetic parameters were evaluated in S.D rat. Compound **56i** exhibits excellent oral absorbance at a dose of 10 mg/kg with a maximum plasma concentration (C_{max}) of 9.05 μg/mL and area under the curve (AUC) of 116 hr.μg/ml. Compound **56i** also possesses very good half-life ($T_{1/2}$) of 10 hr and T_{max} of 5.3 hr. These results indicate that compound **56i** exhibits favorable pharmacokinetic profiles (Table 19).

Table 19: Pharmacokinetic parameters[a] of compound **56i** in S.D. rats at 10 mg/kg oral

Compound	**T_{max}** (hr)	**C_{max}** (μg/ml)	**$T_{1/2}$** (hr)	**AUC (0-inf)** (hr.μg/ml)
4508	5.33 ± 0.42	9.05 ± 1.09	10.24 ± 2.50	115.88 19.43

[a]Values indicated are the mean of n=6 animals and $p < 0.05$ vs vehicle control.

3.3.5 Molecular Docking Study

For a better understanding of the activity of **56i** at molecular level, docking simulations were carried out for this compound using Glide version 5.6, the automated docking program implemented in the Schrodinger package. The geometry of compound docked was subsequently optimized using the LigPrep version 2.6. The complexed X-ray crystal structure of the ligand binding domain (LBD) of PPARα with GW409544 (1K7L.pdb), PPARγ with Rosiglitazone (2PRG.pdb) and PPARδ with GWO742 (3TKM.pdb) were obtained from RCSB Protein Data Bank.

Compound **56i** when docked into PPARα and PPARγ binding pockets adopts a conformation that allows the carboxylic group to form hydrogen bond with Tyr 464 and Ser 289 respectively. Whereas in PPARδ binding pocket the carboxylic group formed hydrogen bonds with Tyr 437, His 413 and His 287. These results support the PPARδ selectivity of Compound **56i** observed in *in vitro* assay (Figure 25).

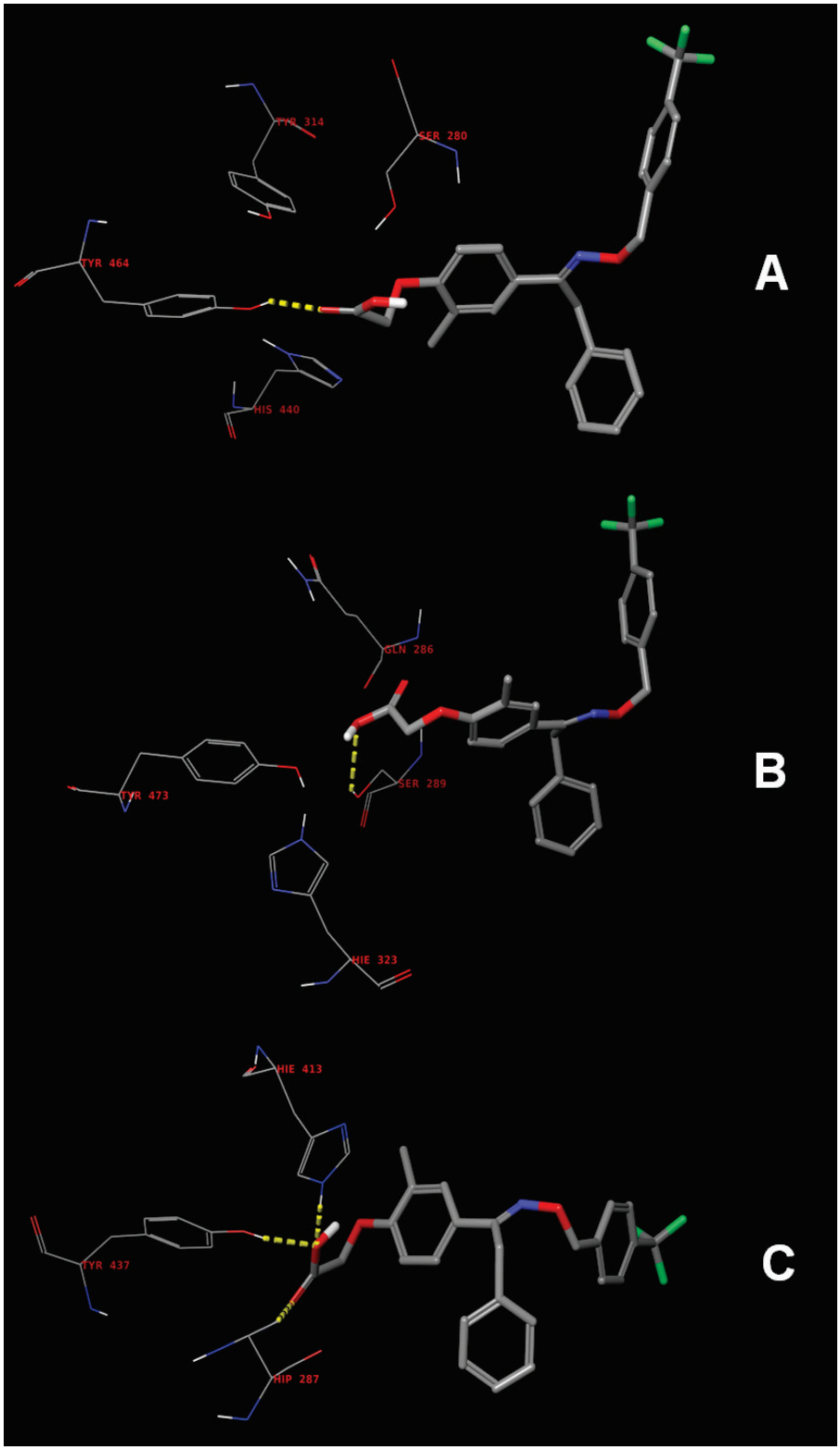

Figure 25: Molecular docking of Compound **56i** into PPARα (A), γ (B) and δ (C) binding pockets: H-bond interactions with amino acids are shown in dashed lines

3.4 Conclusion

In order to achieve the goal of identifying a PPARδ selective agonist, in this chapter the work on design and synthesis of three different series of compounds hd been included. All the compounds were tested for *in vitro* PPAR agonistic activity and *in vivo* studies, pharmacokinetic studies as well as molecular modeling studies were carried out for the most active compound **56i**.

Bearing in mind the results the following conclusions are drawn.

- The compound **56i** was discovered to be a selective and partial PPARδ agonist which exhibits a prominent anti-inflammatory activity without disturbing metabolic levels.
- During *in vitro* it was observed that
  - Substitutions on oxime are sensible for PPAR subtypes selectivity.
  - Bulkier aryl substitution on oxime linker is favorable for PPARδ selectivity whereas substitutions with cycloalkyl and heterocyclic group decrease selectivity.
  - 4-Trifluoromethylbenzyl group as a lipophilic part is the most suitable in terms of PPARδ selectivity compared to benzyl group with another substitutions and heterocyclic group in this scaffold.